




# Pilot-Scale Test of Flue Gas Recirculation for The Silicon Process

Vegar Andersen<sup>1</sup>  · Ingeborg Solheim<sup>2</sup> · Heiko Gaertner<sup>2</sup> · Bendik Sægrov-Sorte<sup>2</sup> · Kristian Etienne Einarsrud<sup>1</sup> · Gabriella Tranell<sup>1</sup>

Received: 31 May 2022 / Accepted: 5 December 2022 / Published online: 20 December 2022  
© The Author(s) 2022

## Abstract

Flue gas recirculation (FGR) for the silicon process may facilitate increasing the CO<sub>2</sub> concentration in the off-gas, which will be beneficial for potential future carbon capture. Lower oxygen concentration in the combustion gas will also reduce NO<sub>x</sub> emissions. An existing 400 kVA Submerged Arc Furnace (SAF) pilot setup was modified to be able to recirculate flue gas and equipped with gas analysis to monitor both the flue gas and the mixed combustion gas entering the furnace. Over a running period of 80 h, including 32 h of startup, twelve different combinations of FGR ratios and flow rates were tested using typical industrial raw materials. Increased CO<sub>2</sub> flue gas concentrations were successfully demonstrated with concentrations over 20 vol % CO<sub>2</sub>. Emissions of NO<sub>x</sub> were shown to be reduced when isolating stable comparable periods within each tapping cycle.

---

The contributing editor for this article was Mansoor Barati.

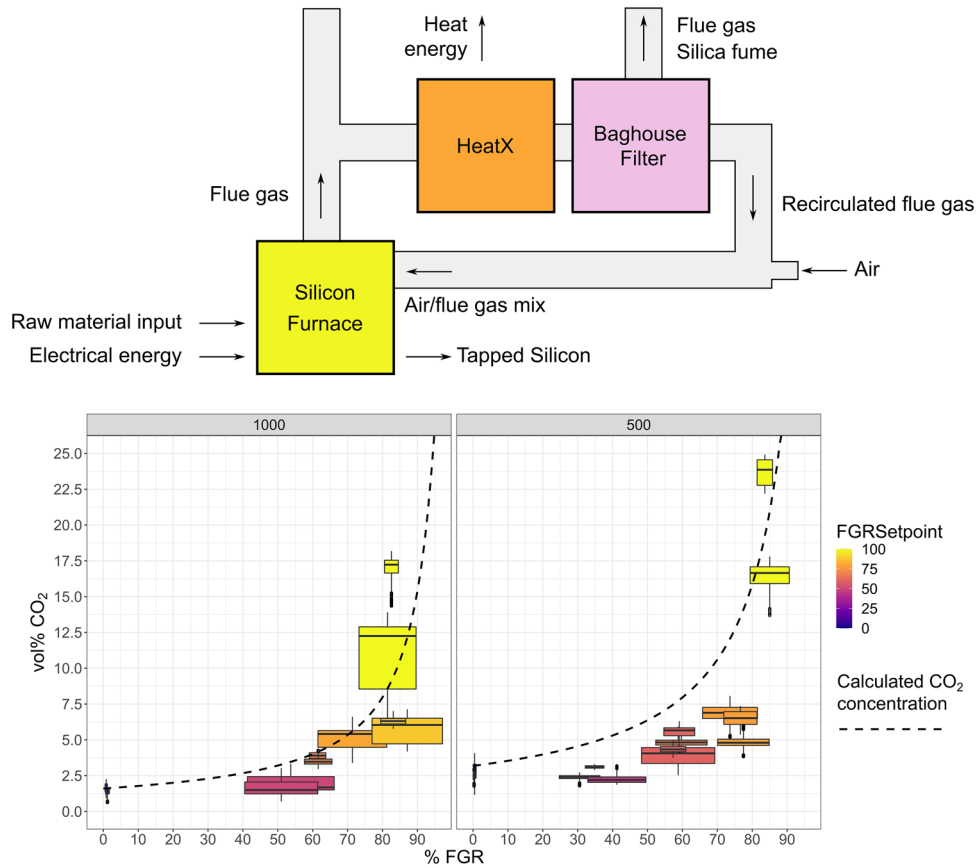
---

✉ Vegar Andersen  
vegar.andersen@ntnu.no

<sup>1</sup> Norwegian University of Science and Technology,  
Trondheim, Norway

<sup>2</sup> SINTEF Industry, Trondheim, Norway

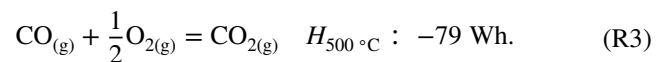
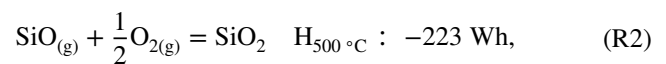
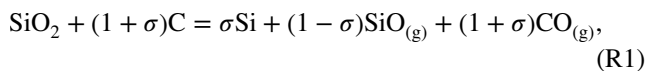
## Graphical Abstract



**Keywords** Silicon · Flue gas recirculation · Silicon production off-gas

## Introduction

Silicon is an essential element that is used in many of the products of modern society such as electronics, silicones, and for alloying other metals. So far, the only industrial way of producing silicon is through carbothermal reduction, where quartz is reduced to silicon with carbonaceous reductants at high temperatures in a submerged arc furnace according to Reaction 1. The silicon alloy is tapped from the bottom of the furnace, while the combustible gases silicon monoxide (SiO), and carbon monoxide (CO) combusts in the furnace hood. This combustion is the source of the byproduct silica fume and CO<sub>2</sub> as shown in Reactions 2 and 3. A detailed description of production of high-silicon alloys can be found in the work of Schei et.al. [1]



The distribution between SiO gas and CO gas from the process is given by the silicon yield  $\sigma$ , as expressed by Reaction 1. In addition to the combustion of process gas, volatile organic compounds (VOC) from the raw material will also combust to form H<sub>2</sub>O, CO<sub>2</sub>, and other gas species, adding to the total emissions. The theoretical minimum CO<sub>2</sub> emission for a metallurgical grade silicon (MG-SI) production with pure carbon reductants and 100% silicon yield is approximately 3.14 kg CO<sub>2</sub>/kg Si. However, depending on silicon yield, the raw materials, and the operational loss of carbon, the actual direct emissions are usually around 5 kg CO<sub>2</sub> per kg of Si, excluding indirect emissions from electricity production. Sævarsdottir et. al [2] estimated the total emission

of CO<sub>2</sub> equivalents from quartz mine to cast metallurgical grade silicon to be in the range from 10.2 to 12.6 kg CO<sub>2</sub> per kg of Si on average. This estimate does not include mining and transportation, and there is also a large variation depending on the source of electrical power. While thermal coal power generation adds from 15 to 21 kg CO<sub>2e</sub>/kg Si to the direct emissions, using renewable sources would be significantly lower. Using the USGS estimate for total silicon and ferrosilicon production in the world of 8 500 000 MT [3] for 2021, the total emission of CO<sub>2e</sub> for the silicon industry is in the order of 100 MT CO<sub>2e</sub> per year.

Since no alternative emission-free production routes for silicon have been commercialized, the industry has been looking at improvements to decarbonize the current carbothermal process. While increased use of biocarbon reduces the emissions of fossil CO<sub>2</sub>, carbon capture and storage (CCS) can reduce the environmental impact of producing silicon by preventing carbon dioxide from entering the atmosphere. Mathisen et al. [4] assessed the opportunity for carbon capture for the Norwegian silicon industries through a techno-economic investigation. Low concentration of CO<sub>2</sub> in the off-gas was one of the challenges identified, resulting in a high capture cost. Of the two plants investigated, one plant had an off-gas containing 1% CO<sub>2</sub>, while the other operation had a concentration of 4%. Mathisen et al. suggested that flue gas recycling (FGR) could be a way of increasing CO<sub>2</sub> concentration, thereby decreasing capture cost. Another benefit of increasing the concentration of CO<sub>2</sub> in the off-gas is making other capture technologies viable. With the current production process, giving a CO<sub>2</sub> concentration up towards 5% vol CO<sub>2</sub>, amine-based scrubber–stripper processes seem to be a good fit. However, other capture technologies become viable options with sufficiently high CO<sub>2</sub> concentrations. One alternative is the CarbFix method, where CO<sub>2</sub> is dissolved in water and injected into suitable basalt geological formations at high pressure. Snæbjörnsdóttir et al. described this process in their review paper [5] and also showed that the marginal capture cost drop under 100 USD\$ once the off-gas CO<sub>2</sub> concentration exceeds 8 vol %.

Flue gas recycling is the concept of recirculating some of the combusted gases back to the process. Flue gases are mixed with combustion air and introduced into the furnace. This is a well-established emission control strategy for reducing NO<sub>x</sub> emissions formed during combustion [6, 7]. FGR can also be used in oxy-fuel combustion processes to avoid excessively high temperatures in the combustion zone, such as optimizing coal power plants for carbon capture [8]. NO<sub>x</sub> formation in the silicon process has been described by Kamfjord [9] and Panjwani et al. [10], who also showed theoretically a substantial potential for NO<sub>x</sub> reduction using FGR [11].

Conventional silicon submerged arc furnaces have a semi-closed hood to capture the flue gases. The fume hood is

operated at pressures lower than atmospheric pressure. Due to the pressure gradient, an excessive amount of ambient air is drawn into the furnace hood, thereby ensuring that the combustion process is contained to the hood and off-gas system. Dilution with fresh air results in off-gas rich in oxygen and nitrogen, but dilute CO<sub>2</sub> concentrations. Reducing the amount of gas extracted from the furnace and thereby reducing dilution with air is the most effective way of increasing CO<sub>2</sub> concentrations but will be limited by either high off-gas temperature or loss of process containment.

With decreasing off-gas extraction, smoke and process gases would at some point start to leak out of openings in the hood. Closing the furnace has been investigated by both Elkem in the 1980s [12] and by Dow Chemical in the 1990s [13] with mixed results, and currently almost all industrial silicon is produced in conventional furnaces with semi-closed hoods. For open processes where the process gas is combusted, the maximum off-gas temperature is primarily limited by the downstream processes. Baghouse filtration, commonly used in silicon production, is usually limited to an off-gas temperature of around 250 °C. Installing a heat exchanger/boiler between the furnace and the filter is a solution which allows higher off-gas temperatures, but at some point, the maximum off-gas temperature would be limited by fouling problems in the off-gas system between the furnace and boiler, especially with regard to the high dust concentration in the off-gas from silicon production. Flue gas recirculation could, therefore, be a potential solution for bridging the gap between a semi-closed and a fully closed furnace to increase the CO<sub>2</sub> concentration in the off-gas and optimizing the process for carbon capture. In the current work, the described pilot experiments are designed to investigate how flue gas recirculation could affect the silicon production process.

## Experimental Setup

Testing the effects of FGR for silicon production was done in a one-phase pilot-scale furnace at the Norwegian University of Science and Technology (NTNU) in Trondheim, Norway.

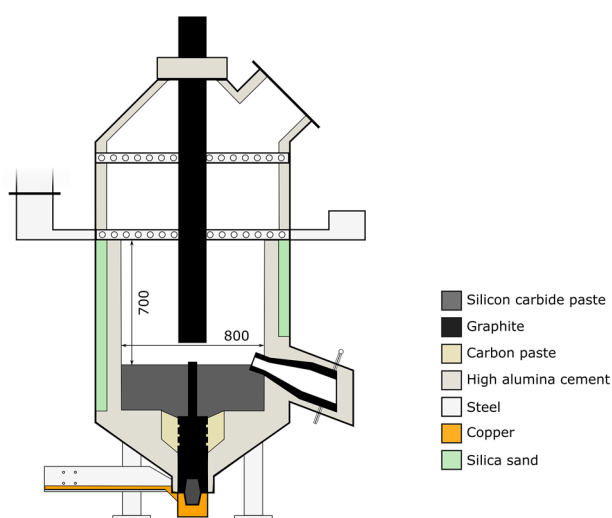
An experimental matrix with two different flow rates and six different FGR rates for each flow was planned and is shown in Table 1. The FGR rate was here defined as the ratio of flue gas to the total gas going into the furnace hood. A broad matrix with several FGR rates was selected to get an overview of which settings could be applicable for the industry and to test that was possible to achieve with the equipment in use. The experiment was a continuous 3-day run with discontinuous tapping. Each tapping cycle, of roughly 1.5 h, was one separate experimental step. When comparing different steps, only the stable part of the tapping cycle was included. Observations as temperatures within operational

**Table 1** Experimental matrix

Exp ID	Flow rate [Nm <sup>3</sup> /h]	FGR rate [%]	Parallels completed
1	1000	0	3
2	1000	50	2
3	1000	70	2
4	1000	80	1
5	1000	88	2
6	500	0	3
7	500	45	3
8	500	60	3
9	500	70	1
10	500	78	3
11	1000	100	2
12	500	100	2

range, normal silica fume generation, and minimal concentration transients defined the stable part of operation. The period right after charging was a transient period where gas composition stabilized, while the end of the cycle was usually dominated by a collapsing charge and excessive blowing. These periods were omitted in the comparison since the process variations influenced the results more strongly than the different FGR rates of the experimental matrix.

The pilot furnace was lined with a monolithic high alumina refractory side lining and a silicon carbide bottom lining, as illustrated in Fig. 1. Tapping was done through a carbon block-tapping portal, using either iron rods in combination with sledgehammers or a heavy-duty drill to open the taphole.

**Fig. 1** Schematic illustration of furnace body and hood. Reproduced from [14]

Electrical power was supplied through a 400 kVA electrical supply through a 6" graphite electrode of EG90 quality, delivered by Tanso. The target electrical load was 160 kW, based on experiences with previous experiments [15], but in several cases had to be reduced to limit the temperature of the off-gas. Variations in electrical resistance and latency in electrode regulation also contributed to deviations in load. In practice, a setpoint for current was entered into the power supply, and the corresponding resistance, to achieve the right load, was adjusted by manually moving the electrode to the right height.

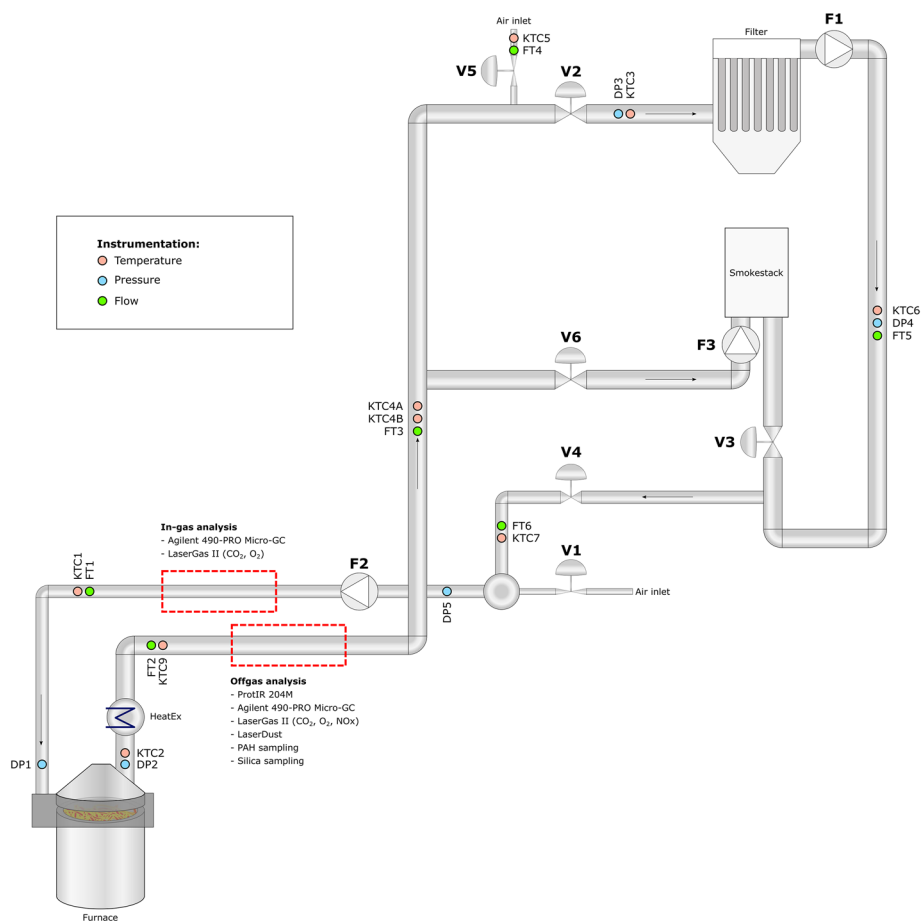
A mix of industrially used raw materials was supplied by a domestic silicon producer. Proximate and ultimate analysis of the raw materials was performed by ALS Scandinavia and details of each material are shown in Table 2. Note that the moisture values were measured in Trondheim by NTNU right before the experiment. The woodchips were dried in a heating cabinet at 100 °C for 24 h before use, while the other materials were used as received. Raw materials were premixed and added after each tapping from the top openings of the furnace. Before adding new raw materials, the charge was stoked with pneumatic chisels to break up crust formations. Carbon coverage was 100% after the initial filling of the furnace, which corresponds to a two-to-one FixC to SiO<sub>2</sub> mole ratio.

Figure 2 shows the off-gas system for the experiment. The off-gas system was modified to extract combusted process gas from the furnace hood, remove particulate matter through a baghouse filter, and distribute the gas either back to the furnace or to the smokestack, depending on the desired FGR rate. Pneumatically controlled butterfly valves were used for directional control, and fan F2 was installed to overcome the pressure drop in the recirculation line. A 4-m-long double pipe heat exchanger cooled the off-gas before the analysis station. After gas analysis, a baghouse

**Table 2** Compositions of raw materials used for the experiment

		Coal	Charcoal	Coke	Woodchips
Share of C-coverage	% of FixC	40	15	30	15
<i>Compound</i>					
Moisture	%	10.8	4.7	11.7	4.8
FixC	% DW	57.6	79	90.5	14.6
Volatiles	% DW	40.4	17.7	6.64	84.2
Ash	% DW	2.04	3.32	2.84	1.16
<i>Elements</i>					
Carbon	% DW	78	83	89.3	50.7
Nitrogen	% DW	1.58	0.39	1.78	0.2
Oxygen	% DW	12	9.6	3.83	41.4
Hydrogen	% DW	5.79	3.71	1.83	6.48
Sulfur	% DW	0.52	<0.1	0.42	0.11

**Fig. 2** illustration of the off-gas system. Valves are denoted V# and fans are denoted F#. Instrumentation placement is also shown, where pressure sensors are marked DP#, temperature measurements KTC#, and flow measurements FT#. Reproduced from [14]



filter removed particulate matter before the gas was directed either to the smokestack or back to the furnace. The baghouse filter was operated with a maximum off-gas temperature of 180 °C, which turned out to be a limiting factor for the length of some experimental steps. Emergency ventilation to the smokestack through valve 6 was implemented as a safety feature and used when temperatures exceeded the operational limit. Enclosure of the furnace hood was done by installing a distribution manifold over the already semi-closed hood. The furnace, combustion hood, and parts of the off-gas system are illustrated in Fig. 3.

Permanent openings in the furnace hood were closed, and with the manifold mounted to the furnace hood, the system was in principle closed. Baghouse cleaning with pressurized air pulsing was only performed in periods of charging and stoking, to avoid adding more air than necessary. Tapping gas was directed into the same off-gas system but was only open in the short periods of tapping. Air was added to the system through the air inlet close to V1. Adding air here was done to make sure that air and flue gas were well mixed before entering the combustion hood.

Although efforts were made to make the system as sealed/gas tight as possible, air leakage into the system was observed. Purging of measuring instruments added

approximately 0.6 Nm<sup>3</sup>/h N<sub>2</sub> gas and 2.4 Nm<sup>3</sup>/h of air. Leakages of fresh air into the filter and through valves were considerably larger and estimated to be in the range

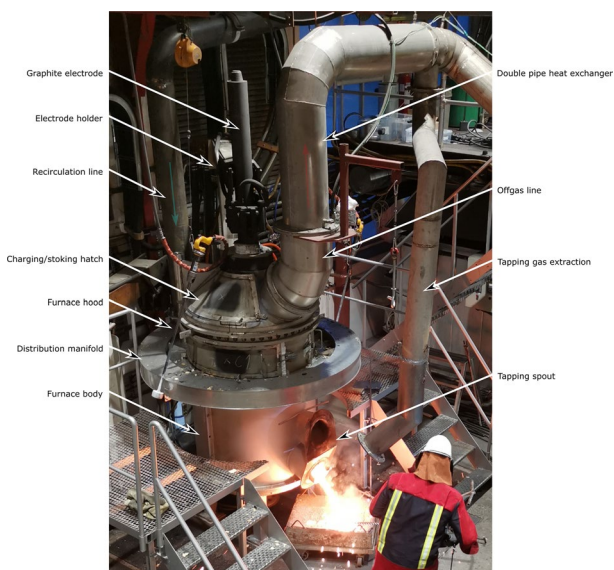


**Fig. 3** Picture of the furnace and parts of the off-gas system during tapping. Reproduced from [14]

of 5 to 10% of the total flow at the highest FGR rates, calculated from the dilution of  $\text{CO}_2$  at the off-gas analysis point to the inlet gas analysis point. The furnace hood was lined with refractory material and had to have large hatches to be able to access the furnace for charging and stoking, which proved hard to get airtight. To limit the leakage into the hood, pressure sensors DP1 and DP2 were placed close to the hood so that fans F1 and F2 could be operated at loads giving as close to ambient pressure as possible in the hood itself. The same principle was applied to limit air leakage in the baghouse filter.

Both the off-gas and the in-gas were analyzed during the experiment. Off-gas was analyzed with an Agilent 490-PRO Micro-GC, ProtIR 204 M combustion gas analyzer, and LaserGas II instruments for measuring  $\text{CO}_2$ ,  $\text{O}_2$ , and  $\text{NO}_x$ . Dust in the off-gas was measured with a LaserDust instrument. Inlet gas was analyzed with another Agilent 490-PRO Micro-GC and two LaserGas II instruments, measuring  $\text{CO}_2$  and  $\text{O}_2$ . Both LaserGas and LaserDust instruments were from NEO Monitors. In addition, isokinetic sample extraction of silica particles and sampling for PAH analysis were performed on the off-gas line.

The Agilent 490-PRO Micro-GCs used the Pro-Station and Soprane II software to quantify  $\text{H}_2$ ,  $\text{O}_2$ ,  $\text{N}_2$ ,  $\text{CO}_2$ ,  $\text{CH}_4$ , and  $\text{CO}$  ( $\text{C}_2\text{H}_4$ ,  $\text{C}_2\text{H}_6$ ,  $\text{COS}$ ). The GC was equipped with two columns to separate the gas constituents and thermal conductivity detectors (TCD) to quantify the gas species. Channel 1 was equipped with a 3 m + 10 m MS5A, RTS column (Serial Nr CM20511010). Channel 1 is operated with Ar carrier gas at a pressure of 22 psi and a temperature of 110 °C. Channel 1 was back flushed after 7 s. Channel 2 is equipped with a 10 m PPQ column (Serial No: CM21011005) and operated with He carrier gas at 22 psi and a temperature of 70 °C.

The inlet, injectors, and backflash module are kept at 90 °C. The injection time was 50 ms for both channels.

Span gas mixtures, instrument Argon 5.0, Helium 6.0, and ambient air were used to calibrate GC and the ABB instrument assuming linear response. The AGA Cylinder

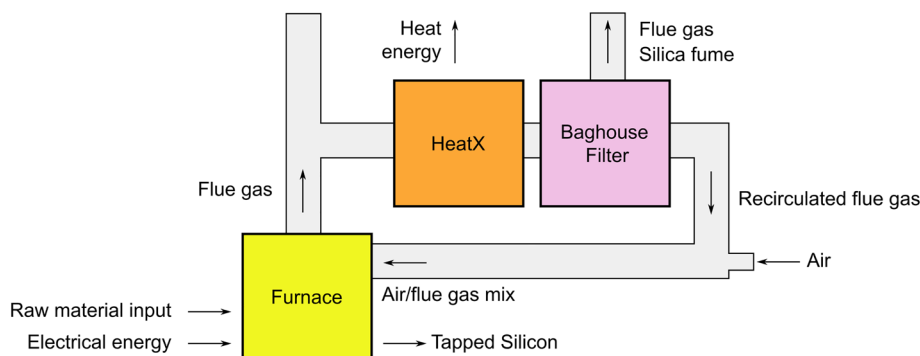
Nr: 750090001972/Certificate No.: 100438851 was used as span gas calibration, containing 20 mol% ( $\pm 2\%$ ) of the reference gases hydrogen, carbon monoxide, carbon dioxide, and methane (Ar balance).

The ProtIR 204 M FTIR analyzer runs Protea Analyser Software (PAS) using the Protea combustion model with pre-defined analysis routines for 20 common combustion gases. The FTIR was used to quantify among others,  $\text{CO}$ ,  $\text{CO}_2$ , and  $\text{NO}_x$ . An on-board zirconia sensor provided oxygen concentration results.

An energy and mass balance model was also set up for the system in HSC-SIM [16]. A simplified flowsheet is shown in Fig. 4. Using the analysis of the raw materials, shown in Table 2, and achieved operational setpoints for the furnace described in the results section, the expected  $\text{O}_2$  and  $\text{CO}_2$  concentrations were calculated at different flue gas flow rates and FGR rates. Combustion of process gas was assumed to run to equilibrium, where the ultimate analysis of each raw material dictates the composition of the resulting off-gas concentration. Note that the FixC content governs the consumption of each raw material, while the total carbon content gives the total emission of carbon from the process. Carbon in the volatile part of the materials is assumed to combust  $\text{CO}_2$  at the charge surface. The energy of each raw material input was estimated using the Dulong equation [17], based on the ultimate analysis of each raw material. Since the model estimates steady-state conditions, a constant supply of raw materials forms the basis of all calculations. Estimations of off-gas concentrations from a silicon plant have been described earlier by Andersen et al. [15] using a similar model, which is a good source of reference for a more detailed description of how the model is set up.

Analysis, processing of the data for the experiment and most of the figure plotting were done using R [18] and the ggplot2 package [19]

**Fig. 4** Simplified flowsheet for steady-state HSC model for flue gas concentrations



## Results and Discussion

Over the course of the almost 80 h long experiment, 27 experimental steps were completed. A total of 7725 kWh electrical energy was used, where 725 kWh was used for baking the lining and 1075 kWh for heating during filling the furnace with raw materials and starting the process, leaving 5925 kWh distributed over 48 h for the actual production process. This gives an average load of 123 kW, well below the set point of 160 kW, which partly is explained by the down-time during tapping and charging. However, due to high temperatures in the off-gas system, the load was often reduced to reduce heat load. Load variations were also caused by varying electrode resistance and regulation latency. The average load in the periods of stable operation was 136 kW.

A total of 176.3 kg of silicon was tapped, and 65.41 kg of silica fume was collected in the baghouse filter. The total quartz consumption ended up at 800 kg for the full experiment, where 200 kg was used to fill the furnace. With residual raw materials left in the furnace during shut down, the actual consumption was estimated to 600 kg. The average power consumption was 33.6 MWh/MT silicon and 9.9 MWh/MT quartz. The silicon yield, calculated from the amount-tapped Si divided by the amount of Si charged to the furnace as quartz, was 62% after the quartz used for filling the furnace was deducted. Note that some silicon was left in the furnace during shut down. Since a significant amount of silica fume was released directly through the smokestack during periods of stoking, charging, and periods of too high off-gas temperatures, calculating silicon yield with regard to silica fume would give an erroneously high estimate.

### Variations Within Each Experimental Step

In all the steps in the experiment, a general pattern of process operation was seen. Early in the tapping cycle, right after stoking and charging, the flue gas temperature was often too high for the baghouse filter and the flow of flue gas had to be gradually routed from the smokestack to the filter and back to the furnace as the temperatures dropped. Following the initial temperature drop, a stable phase followed, with close to steady-state temperatures and concentrations. At the end of the tapping cycle, dust concentrations started increasing as the available carbon for reacting with SiO gas in the charge decreased. This phenomenon is often called blowing, when jets of SiO gas leave the charge and combust with oxygen. Since this effect dominates over the effect of FGR, the stable phase was considered over when an increasing dust concentration in the off-gas was observed.

Figure 5 illustrates these phases for step 13. Step 13 had a FGR setpoint of 100% and a flowrate setpoint of 1000

Nm<sup>3</sup>/h. In the beginning of the step, the flue gas temperatures are too high for the filter. From the relative time -20, the flue gas was gradually introduced to the filter and routed back to the furnace. At relative time -5, the FGR rate is achieved, and the stable period is considered to begin at relative time 0, when the system has consumed surplus oxygen in the circulating gas. The time from charging to stable operation is called ramp-up time in the following discussion. After close to 25 min of stable operation, the dust concentration increases, and the stable period is considered over. The stable period of Step 13 was ended slightly earlier than the dust concentration would imply, due to the bag house filter clogging up. This required pneumatic cleaning of the filter which introduced fresh air into the system prematurely.

A high yield in silicon production is dependent on a porous charge where the process gas SiO can react with carbon. Ideally, the furnace should be charged continuously to have an even supply of carbon to capture as much of the SiO gas as possible. A tapping cycle of 90 min between charging is longer than ideal for such a small furnace and the period of blowing is unavoidable. Figure 6 a and b show how much of the raw materials are consumed, leaving a large cavity under a top crust formation. Although periods of blowing are not uncommon in industrial furnaces, the pilot setup had limitations handling the high dust load and high temperatures. It was, therefore, concluded that excluding these periods, when comparing different experimental steps, it would be the best way of highlighting the effects of FGR.

### Gas Analysis Results for Different FGR Rates

Figure 7 shows the CO<sub>2</sub> concentration in the off-gas with increasing FGR rate. CO<sub>2</sub> concentration was successfully increased with both flow rates in the experiment. The highest off-gas CO<sub>2</sub> concentration was achieved in the runs with the lower flowrate, which allowed for lower pressure differentials in the system and reduced leakage of fresh air. O<sub>2</sub> levels in the combustion gas entering the furnace hood are shown in Fig. 8. Expected concentrations for CO<sub>2</sub> and O<sub>2</sub>, calculated in the HSC model, are shown as dotted lines in Fig. 7 and Fig. 8. In the boxplots from Fig. 7 to Fig. 9, each bar represents one experimental step, where the width of the bar shows the span of FGR rate, or oxygen concentration in combustion gas, within each step. Note that the achieved FGR rate is not the same as the target FGR rate. Leakage of air into the furnace hood and the baghouse filter is limited how high FGR rates could be achieved. The FGR ratio used in the following figures is based on the dilution of CO<sub>2</sub> from the off-gas to the in-gas.

As seen in Fig. 7, the measured CO<sub>2</sub> concentration is generally lower than the calculated concentration from the steady-state model. Especially for the 500 Nm<sup>3</sup>/h steps, CO<sub>2</sub> concentrations are lower than expected. Parts of this

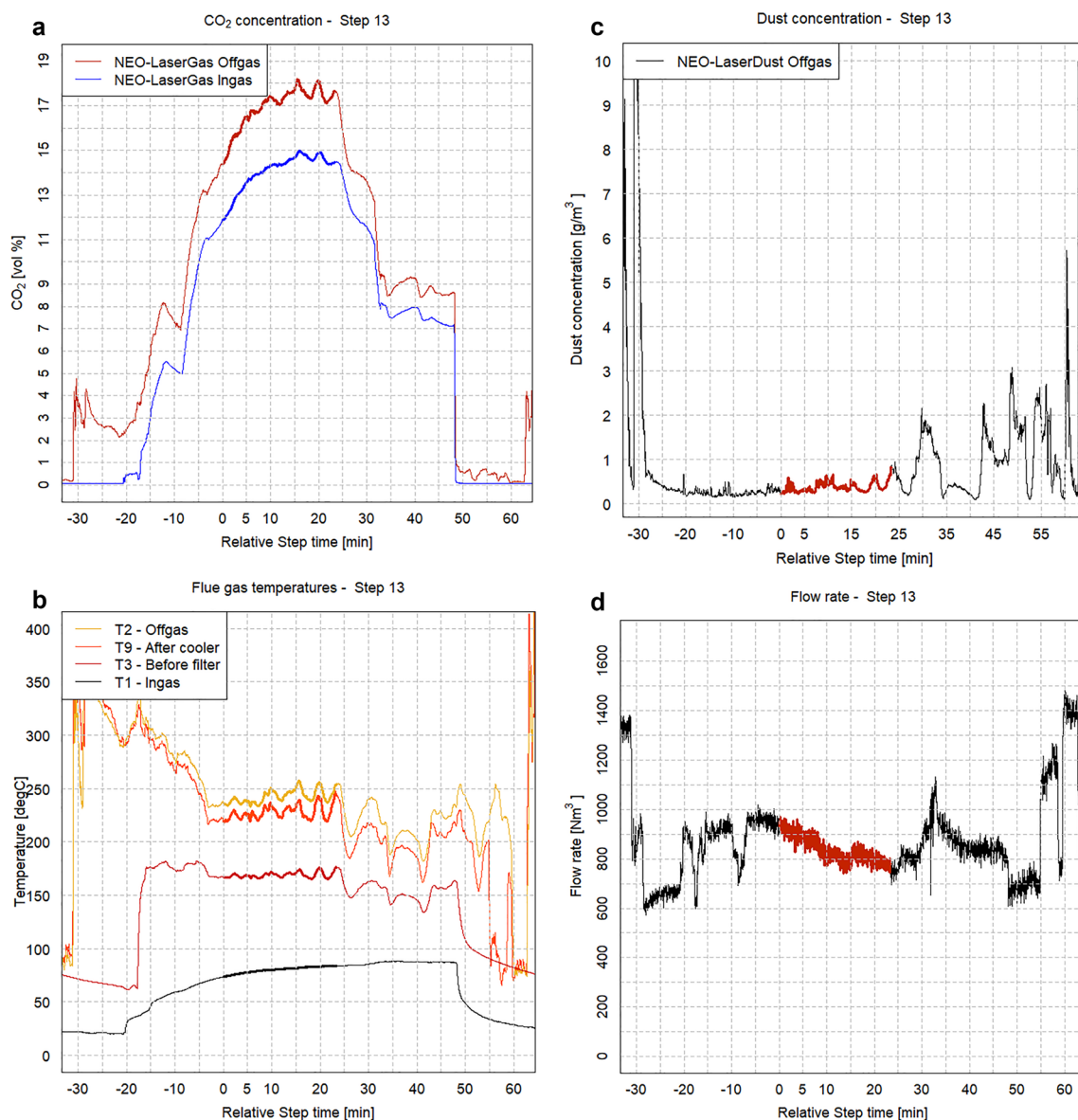


**Fig. 5** CO<sub>2</sub> (a), temperature (b) and dust concentration (c) in the flue gas for step 13, where the FGR setpoint was 100% and the setpoint for flowrate was 1000 Nm<sup>3</sup>/h

can be explained by the steady-state model not including the dynamics of reaching a steady state. The CO<sub>2</sub> from the volatile part of the raw materials is combusted right after charging while the model assumes a constant combustion of volatiles. In this period, the off-gas was directed out through the smokestack due to very high temperatures. This was the case for all the experimental steps and would lead less CO<sub>2</sub> production in the periods where the FGR rates were achieved than the model predicted, since most of the volatiles already had been burned off. Another cause for the deviation from the expected concentrations and the actual results is the leakage of air into the system. While the model includes purge air from the measuring instruments, it did not include any

extra air coming into the system through the furnace hood or the baghouse filter. Relatively, this error would be larger for the 500 Nm<sup>3</sup>/h flow rate steps. Calculated values for oxygen concentrations from the HSC model, hence, generally fit better with the achieved results than for the CO<sub>2</sub> concentrations.

Concentrations of SO<sub>2</sub>, CO, CH<sub>4</sub>, H<sub>2</sub>, and an indicative measure of total organic compounds (TOC) were also measured, and a graphical representation of these gas species can be found in the online supplementary material Figures S1–S5. The average values and maximum and minimum step averages are shown in Table 3 to indicate the order of magnitude and range of these species.



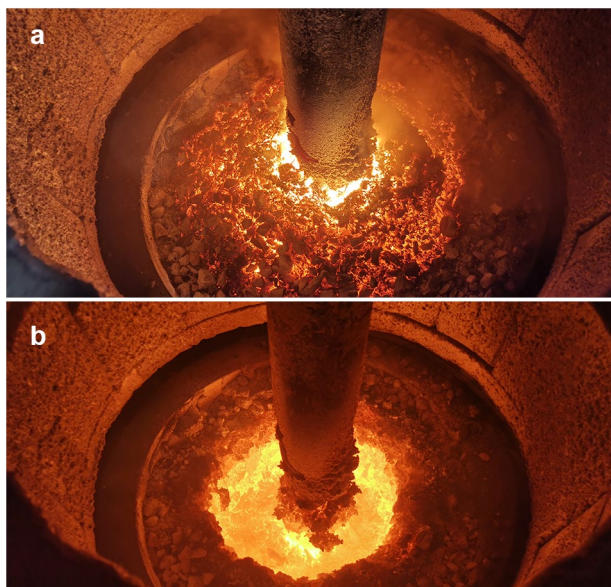


**Fig. 6** **a** Charge surface at the end of a tapping cycle. **b** The same charge surface after stoking with pneumatic chisels to break the crust, revealing the large cavity after consumption of most of the raw materials

SO<sub>2</sub> concentrations were calculated based on the sulfur content in the raw materials as shown in Table 2 and a sulfur yield of 100% to SO<sub>2</sub> in the off-gas. Two studies of sulfur distribution in the silicon process have been published. Myrhaug [20] found a 75% yield of sulfur to off-gas with the remaining sulfur going to silica fume and metal, while Kamfjord [9] found a yield of 96% to the off-gas. For distribution coefficients to species largely going to the off-gas, the coefficients in Kamfjord's study should be more reliable as this study measured gas compositions. In the study by Myrhaug, the only outputs analyzed were silicon and silica fume and the remaining part was assumed to go to the off-gas.

For all steps, the measured SO<sub>2</sub> concentration was significantly lower than that was calculated from the mass balance, assuming all sulfur in the raw materials ended up as SO<sub>2</sub>. Only approximately 10% of the expected concentration was measured. As with the lower CO<sub>2</sub> concentrations, it is more likely that much of the organic sulfur goes to the off-gas following charging, so that only a small amount is captured in the FGR loop. When stable conditions are reached and measuring starts, most of the sulfur has already been driven off. The experimental step at 1000 Nm<sup>3</sup>/h at 82% FGR is illustrated this. This tapping cycle had a longer ramp-up time than the other tapping cycles and shows very low concentration of SO<sub>2</sub> and the trend is similar for the Uncombusted Hydrocarbons (UHC). However, other sulfur-containing species, such as H<sub>2</sub>SO<sub>4</sub> and SO<sub>3</sub>, were not measured, which could explain some of the deviation from the expected SO<sub>2</sub> concentration.

Decreasing O<sub>2</sub> concentration in the combustion air as FGR increases will eventually lead to incomplete combustion. For the experimental steps without any FGR, the concentration of CO gas was in the range of 250 ppm and increased up over 1000 ppm as the oxygen concentration decreased under 10 vol %. Note that some of the CO gas measured here might have been recirculated back to the furnace hood. Since there is no way of knowing how much of the recirculated CO combusts in the hood, and how much freshly formed CO escapes the furnace hood, the concentrations are reported as total CO concentrations in the off-gas. For methane, hydrogen and a measured indicative amount of total organic compounds, the total concentrations in the off-gas are shown without any corrections for FGR. For all these species, there is limited effect of reducing the oxygen content in the combustion air down to 15–16%, before signs of UHC occur at lower oxygen concentrations. Note that step 13, which have a flow rate of 1000 Nm<sup>3</sup>/h and an aim of 100% FGR, did not show an increase in TOC but had a higher than usual ramp-up time. This indicates that a portion

**Fig. 7** CO<sub>2</sub> concentration in off-gas, measured with the NEO LaserGas instruments vs FGR rate. Each column represents an experimental step. Expected CO<sub>2</sub> concentrations calculated for the different FGR rates are shown as the dotted line. Reproduced from [14]

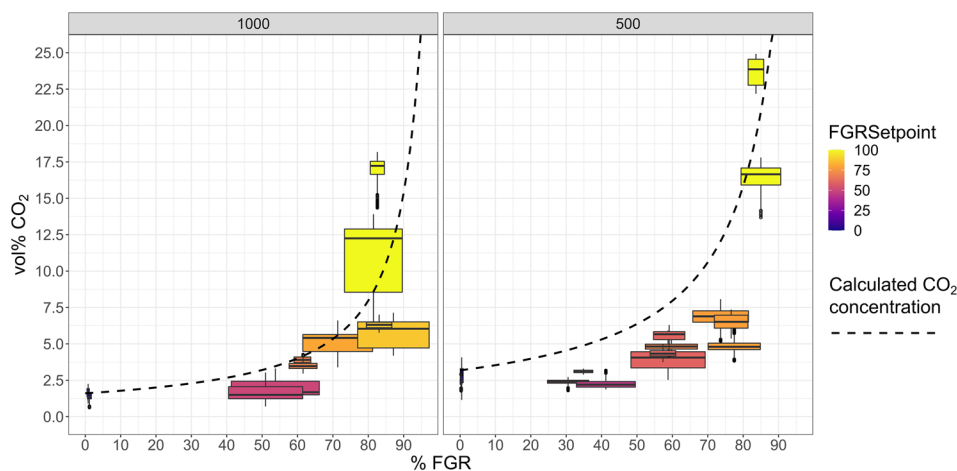


**Fig. 8** O<sub>2</sub> concentration in off-gas, measured with the NEO LaserGas instruments vs FGR rate. Each column represents an experimental step. Expected O<sub>2</sub> concentrations calculated for the different FGR rates are shown as the dotted line. Reproduced from [14]

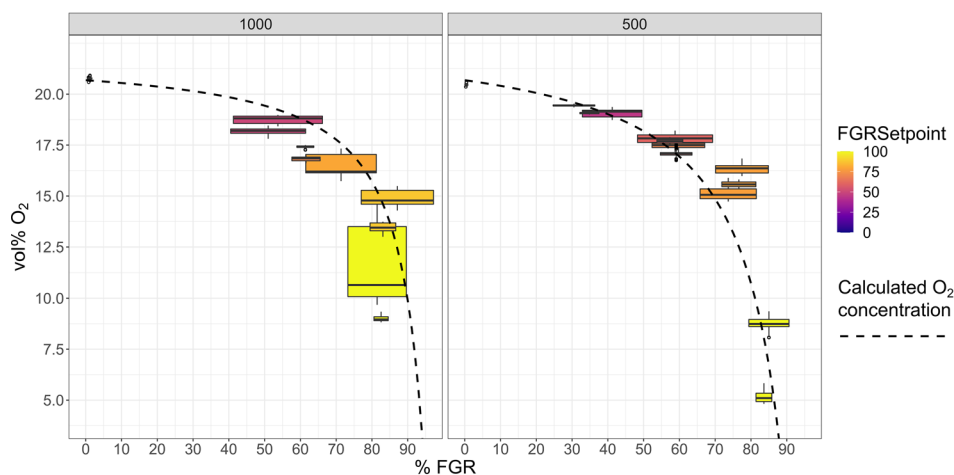


**Table 3** Average concentrations of SO<sub>2</sub>, CO, CH<sub>4</sub>, H<sub>2</sub> and total organic compounds for all tapping cycles as well as the lowest and highest average tapping cycle values, showing the range of concentrations

Gas species	Minimum [vol ppm]	Average [vol ppm]	Maximum [vol ppm]
SO <sub>2</sub>	-	20.2	78.0
CO	154	767	6780
CH <sub>4</sub>	0.908	7.99	127
H <sub>2</sub>	-	0.00323	0.0505
TOC	0.750	5.19	72.9

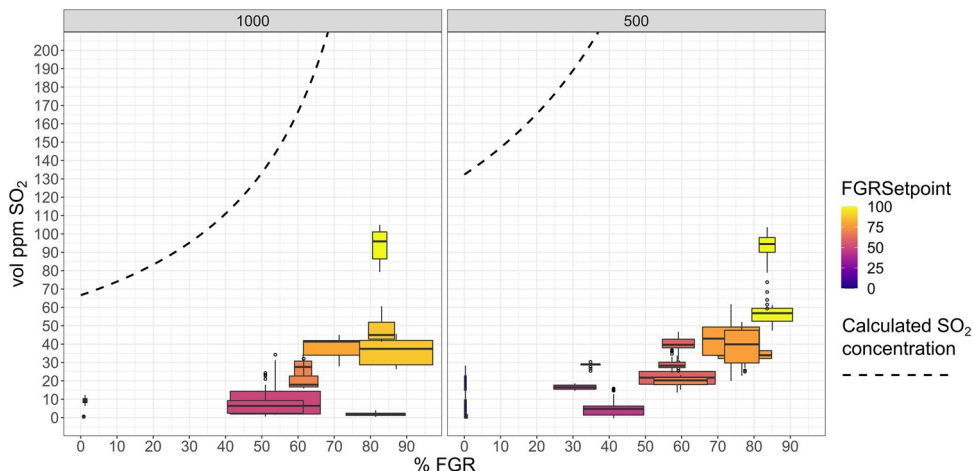
of organic compounds are driven off during the ramp-up time, before FGR has been started.

A decreasing generation of NO<sub>x</sub> was observed with increasing FGR, especially for the steps with 500 Nm<sup>3</sup>/h off-gas flow rate. Fig. 9 shows the NO<sub>x</sub> concentrations measured with the NEO LaserGas instrument. The dotted line is calculated as NO<sub>x</sub> concentration from the HSC model, assuming a constant mass flow of NO<sub>x</sub> from the

furnace equal to average of the zero FGR rate steps. It basically shows how the NO<sub>x</sub> concentration is expected to increase due to less dilution. All 500 Nm<sup>3</sup>/h runs show lower NO<sub>x</sub> concentrations than that would be expected from a constant mass flow and concentration due to recirculation, while this is the case for four out of seven steps for the 1000 Nm<sup>3</sup>/h experiments. This indicates that the NO<sub>x</sub> generation is reduced with increasing FGR rates and further reduced by also limiting off-gas flow.

The NO<sub>x</sub> concentration also appeared to be correlated with the silica fume concentration in the off-gas. The periods with a high concentration of silica fume in the off-gas can be explained by direct blowing of SiO from the crater. For this reason, three experimental steps, where the charge burden collapsed early and caused heavy blowing, have been removed from the comparison in Fig. 9. As SiO combusts in the furnace hood, the high local temperatures would give a high rate of thermal NO<sub>x</sub> production. The same effect was observed by Kamfjord [9] for industrial furnaces and has been modeled by Panjwani [11].

**Fig. 9** NO<sub>x</sub> concentrations measured with the NEO Laser gas instrument vs the FGR rate. The dotted line is the calculated NO<sub>x</sub> concentration given a fixed mass flow from the furnace



## Conclusions and Outlooks

Flue gas recirculation has been successfully used to increase the CO<sub>2</sub> concentration in the off-gas from a pilot-scale silicon process using typical industrial raw materials. Signs of organic compounds' incomplete combustion and other combustible gases increase at oxygen concentrations lower than 15–16 vol % O<sub>2</sub>. For the pilot furnace experiments, no significant increase in CO or TOC, indicating incomplete combustion, was observed by raising the CO<sub>2</sub> concentration in the off-gas from 1.5 to 5 vol % CO<sub>2</sub> for a gas flow of 1000 Nm<sup>3</sup>/h, and from 2.6 vol % to 6.5 vol % for the steps with a gas flow 500 Nm<sup>3</sup>/h.

The off-gas composition calculated with a mass and energy balance model in HSC-SIM is in good accordance with measurement data of the off-gas analyses. Lower measured CO<sub>2</sub> concentrations than those calculated are most likely caused by the effect of combusting and removal of the volatiles during ramp-up period in open loop while the furnace was charged until FGR is initialized. This ramp-up time is a large uncertainty regarding how well the experiment predicts incomplete combustion of volatile organic compounds. Since all steps start at an oxygen concentration of 21% O<sub>2</sub>, a portion of the volatiles that could cause problems with FGR have a chance of combusting at normal oxygen concentration during the ramp-up period. However, the fact that an increase in TOC can be seen in the higher FGR steps indicate that the ramp-up time is short enough to capture at least a portion of UHC from the volatile matter.

The findings of the current study are promising for a partial FGR approach for industrial silicon production application. Especially the indication of a reduced NO<sub>x</sub> generation is encouraging. CO<sub>2</sub> concentrations more than 10 vol % could be sufficient to make other carbon capture methods competitive, especially if these methods simplify the gas treatment needed to handle SO<sub>2</sub> and products of incomplete combustion. Further research is needed to investigate the effect of burning/cracking a higher amount of raw material volatiles under high FGR rates, which could lead to more contamination of the silica fume. It would also be interesting to see the effects of higher moisture content in the raw materials. This will give valuable input to evaluating the feasibility of FGR for the silicon production process.

## Future Work

For future FGR experiments, several improvements could be made to the setup. For this experiment, the energy content in the charge mix was too high. The charcoal had a significant content of fines, and the woodchips were dried before use, reducing the moisture content from approximately 50%

down to 4.75%. This resulted in too high off-gas temperatures right after charging where the gas was too hot to handle for the filter and delayed start of the experimental step. The delay in reaching the desired FGR rate leads to losses of combustion products from the volatiles through the smokestack. Combustion of volatiles, together with combustion of charcoal fines, was the cause for the high temperatures, which in turn had to be dealt with by routing the flue gas to the smokestack instead of recycling it through the baghouse filter. Future FGR experiments should aim to limit the peak temperatures to a range which is manageable by the heat exchanger and bag house filter. A more efficient heat exchanger or a more robust baghouse filter is one option. Removal of fines from the charcoal is another option that would reduce the initial temperature peak. Using moist woodchips would also reduce peak flue gas temperature in the early phase of each step, as the evaporation of moisture would coincide with the combustion of volatiles from new raw materials. Having more moisture in the combustion chamber would also make the conditions more alike the conditions prevailing in industrial furnaces. A downside of introducing more moisture is increasing the dewpoint temperature, which would increase corrosion issues, especially on the recirculation line where the off-gas temperature was much lower than the acid dewpoint. Generally, an evaluation of the energy content in the charge composition should be done to match the energy output to the heat tolerance of the system, based on the experience of this experimental campaign. The observed stable operation is limited in the start by high temperatures, but also in the end by excessive blowing. Another way of extending the stable operation phase is to delay the onset of this blowing. This could be achieved by having a higher furnace with a larger upper reaction zone containing more carbon material. Adding raw material during each experimental step could also be an option but would require a valve arrangement to limit the addition of air into the system, which would reduce the FGR rate. This would delay the need for charging new material, but stoking the furnace would still require opening the hood and letting ambient air in.

**Supplementary Information** The online version contains supplementary material available at <https://doi.org/10.1007/s40831-022-00639-0>.

**Acknowledgements** This work has been funded by the research centers FME HighEFF (257632) and SFI Metal Production (237738) and the projects SiNoCO<sub>2</sub>—Silicon production with no CO<sub>2</sub> emissions (269431), PAHssion (295744), as well as the Climit supported project Elkem CCS (620106). The authors gratefully acknowledge the financial support from the Research Council of Norway and the user partners in the involved centers and projects. The authors also declare that they have no conflicts of interest.

**Funding** Open access funding provided by NTNU Norwegian University of Science and Technology (incl St. Olavs Hospital - Trondheim University Hospital). Funding was provided by Norges Forskningsråd

(Grant Nos. 257632, 237738, 269431, and 295744) and Climit (Grant No. 620106).

**Open Access** This article is licensed under a Creative Commons Attribution 4.0 International License, which permits use, sharing, adaptation, distribution and reproduction in any medium or format, as long as you give appropriate credit to the original author(s) and the source, provide a link to the Creative Commons licence, and indicate if changes were made. The images or other third party material in this article are included in the article's Creative Commons licence, unless indicated otherwise in a credit line to the material. If material is not included in the article's Creative Commons licence and your intended use is not permitted by statutory regulation or exceeds the permitted use, you will need to obtain permission directly from the copyright holder. To view a copy of this licence, visit <http://creativecommons.org/licenses/by/4.0/>.

## References

- Schei A, Tuset JK, Tveit H (1998) Production of high silicon alloys. TAPIR, Trondheim
- Sævarsdóttir G, Kvande H, Magnusson T (2021) Greenhouse gas emissions from silicon production -development of carbon footprint with changing energy systems. In: Proceedings of the 16th international ferro-alloys congress 2021, Trondheim, Norway. <https://doi.org/10.2139/ssrn.3926088>.
- U.S. Geological Survey (2022) Mineral commodity summaries—silicon. <https://www.usgs.gov/centers/national-minerals-information-center/silicon-statistics-and-information>. Accessed 10 Feb 2022
- Mathisen A, Normann F, Biermann M, Skagestad R, Haug AT (2019) CO<sub>2</sub> capture opportunities in the norwegian silicon industry. In: TCCS–10. Trondheim, Norway
- Snæbjörnsdóttir SÓ, Gislason SR (2016) CO<sub>2</sub> storage potential of basaltic rocks offshore Iceland. *Energy Procedia* 86:371–380. <https://doi.org/10.1016/j.egypro.2016.01.038>
- Turns S, Haworth DC (2020) An introduction to combustion: concepts and applications. McGraw-Hill, New York
- Clean Air Technology Center and U.S. Environmental Protection Agency (1999) Nitrogen oxides (NO<sub>x</sub>), why and how they are controlled. U.S. Environmental Protection Agency, Research Triangle Park, North Carolina 27711, Technical Bulletin EPA 456/F-99-006R, Nov. 1999.
- Fujimori T, Yamada T (2013) Realization of oxyfuel combustion for near zero emission power generation. *Proc Combust Inst* 34(2):2111–2130. <https://doi.org/10.1016/j.proci.2012.10.004>
- Kamfjord NE (2012) Mass and energy balances of the silicon process. PhD Thesis, NTNU, Trondheim, Norway
- Panjwani B, Olsen JE (2013) Combustion and mechanism of NO<sub>x</sub> formation in Ferrosilicon. Presented at the European Combustion Meeting, June 2013.
- Panjwani B, Pettersen T, Wittgens B (2020) Controlling flue gas temperature from ferro silicon submerged arc furnaces (SAF) using flue gas recirculation (FGR). In: 14th international conference on CFD in oil & gas, metallurgical and process industries, Dec 2020.
- Arnesen AG, Bjørdal J (1981) Split body closed FeSi75 furnace, *Electric furnace Conf* vol 38.pdf.
- Dosaj VD, Brumels MD, Haines CM, May JB (1992) Silicon smelting in a closed furnace. EG and G Idaho Inc., Idaho Falls
- Andersen V, Solheim I, Gaertner H, Sægrov-Sorte B, Einarsrud KE, Tranell G (2022) Pilot scale test of flue gas recirculation for the silicon process. In: REWAS 2022: developing tomorrow's technical cycles, vol I, Anaheim. pp. 555–564. [https://doi.org/10.1007/978-3-030-92563-5\\_58](https://doi.org/10.1007/978-3-030-92563-5_58).
- Solheim I, Jensen R, Kamfjord NE (2012) Equipment for pilot scale experiments of NO<sub>x</sub> emissions from the silicon process. In: 3rd international symposium on high-temperature metallurgical processing. Wiley, New York, pp 33–40. <https://doi.org/10.1002/9781118364987.ch5>.
- Roine A (2020) HSC chemistry. Outotec. <https://www.outotec.com/products-and-services/technologies/digital-solutions/hsc-chemistry/>
- Hosokai S, Matsuoka K, Kuramoto K, Suzuki Y (2016) Modification of Dulong's formula to estimate heating value of gas, liquid and solid fuels. *Fuel Process Technol* 152:399–405. <https://doi.org/10.1016/j.fuproc.2016.06.040>
- R Core Team (2020) R: a language and environment for statistical computing. R Foundation for Statistical Computing, Vienna, Austria. <https://www.R-project.org/>
- Wickham H (2009) ggplot2. Springer New York. <https://doi.org/10.1007/978-0-387-98141-3>.
- Myrhaug EH (2003) Non-fossil reduction materials in the silicon process—properties and behavior. PhD thesis NTNU.

**Publisher's Note** Springer Nature remains neutral with regard to jurisdictional claims in published maps and institutional affiliations.